Carbohydrate Polymers 115 (2015) 617–628

Contents lists available at ScienceDirect

Carbohydrate Polymers

journal homepage: www.elsevier.com/locate/carbpol

Flocculation and adsorption properties of biodegradable gum-ghatti-grafted poly(acrylamide-*co*-methacrylic acid) hydrogels

H. Mittal[a,c,*], R. Jindal[b], B.S. Kaith[b], A. Maity[c], S.S. Ray[a,c,*]

[a] Department of Applied Chemistry, University of Johannesburg, Doornfontein, Johannesburg 2028,South Africa
[b] Department of Chemistry, National Institute of Technology, Jalandhar 144011, Punjab, India
[c] DST/CSIR National Centre for Nanostructured Materials, Council for Scientific and Industrial Research, Pretoria 0001, South Africa

ARTICLE INFO

Article history:
Received 15 July 2014
Received in revised form
10 September 2014
Accepted 11 September 2014
Available online 23 September 2014

Keywords:
Gum ghatti
Hydrogel polymer
Graft co-polymerization
Biodegradation
Flocculation
Adsorption

ABSTRACT

This study reports the microwave-assisted synthesis of gum-ghatti (Gg)-grafted poly(acrylamide-*co*-methacrylic acid) (AAm-*co*-MAA) hydrogels for the development of biodegradable flocculants and adsorbents. The synthesized hydrogels were characterized using TGA, FTIR and SEM. TGA studies revealed that the synthesized hydrogels were thermally more stable than pristine Gg and exhibited maximum swelling capacity of 1959% at 60 °C in neutral pH. The optimal Gg-cl-P(AAm-*co*-MAA) hydrogel was successfully employed for the removal of saline water from various petroleum fraction–saline emulsions. The maximum flocculation efficiency was achieved in an acidic clay suspension with a 15 mg polymer dose at 40 °C. Moreover, the synthesized hydrogel adsorbed 94% and 75% of Pb^{2+} and Cu^{2+}, respectively, from aqueous solutions. Finally, the Gg-cl-P(AAm-*co*-MAA) hydrogel could be degraded completely within 50 days. In summary, the Gg-cl-P(AAm-*co*-MAA) hydrogel was demonstrated to have potential for use as flocculants and heavy metal absorbents for industrial waste water treatment.

1. Introduction

In the past two decades, the demand for polymer-based materials has increased considerably because of their user-friendly nature, low cost, ready availability and, most importantly, their properties can be easily modified to suit the nature of the application. The polymer industry has undergone tremendous growth, and the polymer-based materials have found applications in various fields, such as biomedical applications, spare parts for the automobile industry, food packaging and serving materials, computer hardware parts and even water purification applications (Siracusa, Ingrao, Giudice, Mbohwa, & Rosa, 2014; Srivastava, O'Connor, Pandit, & Wall, 2014; Zah, Hischier, Leão, & Braun, 2007). Generally, polymer-based materials leave behind a large amount of solid waste that is not easy to recycle. Biodegradation is the process of the deterioration of the physico-chemical properties of polymers and the reduction of the matrix molecular masses by converting them into CO_2, H_2O and CH_4 under the action of enzymes and/or the chemical decomposition associated with living organisms (bacteria, fungi, yeasts and insects) or their secretion products, and the residues that remain after biodegradation should be non-toxic in nature (Raul Muñoz & Benoit Guieysse, 2006; Ashori, 2008; Nayak, 2000; Suvorova, Tyukova, & Trufanova, 2000; Wang, Yang, & Wang, 2003). In recent years, Gum polysaccharides biodegradable have attracted considerable attention because of their unique features, including low cost, ready availability, biocompatibility and an eco-friendly nature. The primary disadvantage of gum polysaccharide-based polymers is their poor mechanical properties compared with those of non-biodegradable polymers. The graft co-polymerization of gum-polysaccharides with vinyl monomers is the widely studied modification technique to improve their inherent properties. (Alvarez-Manceñido, Landin, Lacik, & Martínez-Pacheco, 2008; Guo, Ge, Li, Mu, & Li, 2014; Malik, Kumar, & Ahuja, 2012; Mittal, Ballav, & Mishra, 2014; Shi & Zhang, 2007; Shi, Wang, & Wang, 2011; Xu, Luo, Lin, Zhuo, & Liang, 2009).

Flocculation is a very efficient technique for the purification of domestic/industrial potable water. Flocculants can be either inorganic additives or macromolecular compounds. Flocculants based on macromolecular compounds are preferred over inorganic additives because their molar mass, chemical structure, charge density and the nature of their functional groups can be easily modified.

* Corresponding authors at: University of Johannesburg, Applied Chemistry, Neend Street, Doornfontein, Johannesburg 2028, Gauteng, South Africa. Tel.: +27 847067375; fax: +27 128412229.
E-mail addresses: mittal.hemant5@gmail.com (H. Mittal), rsuprakas@csir.co.za (S.S. Ray).

http://dx.doi.org/10.1016/j.carbpol.2014.09.026
0144-8617/

Furthermore, a very small amount of polymer-based flocculent is required compared with mineral flocculants. Synthetic polymer-based flocculants demonstrate better efficiency compared with natural flocculants but they are toxic and non-biodegradable in nature (Gaudreault, Cesare, Weitz, & van de Ven, 2009; Singh et al., 2000). Recently, a great deal of effort has been made toward the development of flocculants with the advantages of both natural and synthetic polymers (Mittal, Fosso-Kankeu, Mishra, & Mishra, 2013a; Ghimici & Nichifor, 2010, 2012; Ghimici, Constantin, & Fundueanu, 2012; Ho, Norli, Alkarkhi, & Morad, 2010; Rani, Sen, Mishra, & Jha, 2010; Wan, Li, Wang, Chen, & Gu, 2007).

Gum ghatti (Gg), a complex polysaccharide, is an exudate of the *Anogeissus latifolia* tree, which belongs to the *Combretaceae* family. It is a common additive in food, where it serves as a thickening agent and a preservative. Aspinall (1980) and Aspinall, Hirst, and Wickstrom, (1955) have extensively studied the structure of Gg and found to have an extremely complex structure composed of sugars such as L-arabinose, D-galactose, D-mannose, D-xylose and D-glucoronic acid in a 48:29:10:5:10 molar ratio. Gg contains alternating 4-*O*-subsituted and 2-*O*-subsituted α-D-mannopyranose units and chains of 1 → 6 linked β-D-galactopyranose units with side chains that are most frequently single L-arabinofuranose residue (Fig. S1, Supplementary information) (Mittal & Mishra, 2014).

Recently, several researchers have investigated the fabrication of gum-polysaccharides-based graft co-polymers and their biodegradation properties. However, the problem with most of these materials is either their resistance to biodegradation or their poor property profiles. Moreover, graft co-polymerization using conventional methods are highly time consuming and results in a high cross linking density, whereas the microwave-assisted graft co-polymerization technique is very rapid and produces very low cross linking density (Mishra, Sand, Mishra, Yadav, & Behari, 2010; Sand, Yadav, Mishra, Tripathy, & Behari, 2011; Yadav et al., 2012). In this particular study, we sought to gain an understanding of the effect of the microwave-assisted method on the biodegradable nature of Gg-based graft co-polymers and on their other properties, such as flocculation and swelling capacity. Therefore, a hydrogel polymer of Gg with a binary monomer mixture of poly(acrylamide-*co*-meth acrylic acid), i.e., P(AAm-*co*-MAA), was synthesized using the microwave-assisted technique. The biodegradable nature, flocculation characteristics, swelling behavior and adsorption capacity of the synthesized hydrogel polymer were also studied.

2. Experimental

2.1. Materials

Gg, AAm, MAA, *N*,*N*′-methylene-bis-acrylamide (MBA), potassium persulfate (KPS), ascorbic acid (ABC), petroleum ether, lead nitrate, copper sulfate and kaolin were purchased from Merck Chemicals, India. Petrol and diesel were purchased from Indian Oil Corporation Limited, India. All chemicals were of analytical grade and were used as received without further purification. All solutions were prepared in triple-distilled water. Stock solutions of metal ions (1000 mg/l) were prepared by dissolving the appropriate amounts of corresponding metal salts in sterile distilled water and were further diluted with distilled water to prepare the working solutions of the desired concentrations.

2.2. Synthesis of the Gg-cl-P(AAm-co-MAA) hydrogel polymer

The Gg-cl-P(AAm-*co*-MAA) hydrogel polymer was synthesized in microwave reactor using AAm as the principal monomer and MAA as secondary monomer. The reaction conditions were optimized for the synthesis of a hydrogel polymer of Gg with AAm in microwave reactor (Mittal, Kaith, & Jindal, 2010). In brief, the various optimized reaction conditions were time (s) = 90, volume of distilled water (ml) = 10, pH = 7.0, initiator molar ratio (KPS: ascorbic acid) = 1:0.5, MWP (%) = 80, [AAm] (mol/l) = 0.9859, and [MBA] (mol/l) = 0.0974. Before the graft co-polymerization reaction was initiated, 1.0 g of Gg was suspended in 10 ml of distilled water for 12 h to achieve better dispersion of the polysaccharide in water. After 12 h, a mixture of initiators (ascorbic acid and KPS) was added to the reaction vessel under constant stirring. After 15 min, which was assumed to be sufficient to generate free-radical sites on the Gg, a binary monomer mixture of AAm and MAA was added to the reaction vessel under continuous stirring. The concentration of AAm was kept fixed at 0.9859 mol/l, whereas the concentration of MAA was varied from 3.51 to 8.201 mol/l. After the complete dissolution of the binary monomer mixture, the optimized amount of cross linker i.e., MBA (0.0974 mol/l), was added to the reaction mixture. The reaction vessel was placed in the microwave reactor, and the graft co-polymerization reaction was allowed to proceed for 90 s. After the completion of the reaction, the vessel was removed from the microwave reactor and allowed to cool at room temperature. A mixture of homopolymers and the un-reacted copolymer was separated out from the reaction system via Soxhlet extraction with acetone followed by water. Finally, the synthesized graft co-polymer was dried at 50 °C in a hot air oven till a constant weight was achieved. The selection of the best-quality hydrogel polymer for the remaining studies was performed on the basis of the percentage swelling (P_s), which was calculated using the following equation:

$$P_s = \frac{W_s - W_d}{W_d} \times 100 \quad (1)$$

where W_s and W_d are the weights of the swelled and dry hydrogel polymer samples, respectively.

2.3. Characterization

The graft co-polymerization of Gg with the binary co-monomer mixture of AAm and MAA and degradation of the Gg-cl-P(AAm-*co*-MAA) hydrogel polymer were confirmed using FTIR and SEM. The FTIR spectra of the Gg-cl-P(AAm-*co*-MAA) hydrogel polymer before degradation and various stages of degradation were recorded on a PERKIN ELMER RXI spectrophotometer using KBr pellets in the spectral range of 4000–400 cm^{-1} with a resolution of 4 cm^{-1}. The morphologies of the Gg-cl-P(AAm-*co*-MAA) hydrogel polymer at various stages of degradation were studied using scanning electron microscopy (LEO, 435VF, LEO Electron Microscopy Ltd., Germany). All samples were non-conducting in nature; thus they were coated with gold to introduce the conduction capability. The thermal-degradation behavior of Gg after graft co-polymerization with P(AAm-*co*-MAA) was studied using TGA/DTA/DTG (TG/DTA 6300, SII EXSTAR 6000, SII Nanotechnology Incorporation, Japan) in an air environment at a heating rate of 10 °C/min.

2.4. Swelling studies in distilled water

The swelling efficiency (P_s) of the Gg-cl-P(AAm-*co*-MAA) hydrogel polymer was examined at various time intervals (4, 8, 12, 16, 20 and 24 h), temperatures (30, 40, 50, 60 and 70 °C) and pH values (3.0 to 13.0) in distilled water. Several 100 mg samples of hydrogel polymer were immersed in 100 ml of distilled water each. After a certain time interval, the samples were removed, gently wiped and weighed. P_s was calculated using Eq. (1). After the optimization of the swelling time, the temperature of the swelling medium and the pH were optimized to achieve the maximum swelling efficiency.

2.4.1. Swelling studies in different salt solutions

The effect of ionic strength of various cations—Na^+, Ba^{2+}, Fe^{3+} and Sn^{4+}, each of different ionic strengths of 0.01, 0.02, 0.03, 0.04 and 0.05 mol/l, respectively, on the P_s of the Gg-cl-P(AAm-*co*-MAA) hydrogel polymer was investigated in NaCl, $BaCl_2$, $FeCl_3$ and $SnCl_4$ salt solutions, respectively, at the pre-optimized time, temperature and pH in distilled water. Initially, weighed amounts of hydrogel polymer were immersed in the salt solutions of different ionic strengths. After the desired time interval, the samples were removed from the salt solutions, wiped carefully and weighed. P_s was calculated using Eq. (1).

2.5. Biodegradation studies

The biodegradable nature of the Gg-cl-P(AAm-*co*-MAA) hydrogel polymer was examined under controlled moisture conditions using the soil composting method. The detailed procedure can be found in a previous publication (Mittal, Mishra, Mishra, Kaith, & Jindal, 2013b). In brief, hydrogel polymer samples were buried in soil compost collected from the waste water effluent discharge plant of the National Institute of Technology, Jalandhar, India. For these studies, rectangular samples ($2 \times 2 \times 1.5\ cm^3$) were prepared and buried at a 2 cm depth, 3 cm apart from each other, in soil compost in a flower pot. As this waste water effluent discharge plant has been running for past two decades, the soil compost collected from it is rich in microbes. The microbe rich water from the plant was added to the compost on alternating days to compensate for water loss caused by evaporation. The progress of the degradation process was examined every 5 days. After every 5 days, the samples were extracted from the compost, carefully cleaned, dried at 50 °C in a vacuum oven and weighed. The progress of degradation was evaluated by studying the changes in physical appearance, percentage weight loss, morphology and chemical composition of the hydrogel polymer. The percentage weight loss after every 5 days was calculated using the following equation:

$$\text{weight loss}\ (\%) = \frac{W_i - W_t}{W_i} \times 100 \quad (2)$$

where W_i is the initial weight of the hydrogel polymer and W_t is the weight after a particular time interval.

2.6. Selective absorption of saline from various petroleum fraction–saline emulsions

The Gg-cl-P(AAm-*co*-MAA) hydrogel polymer was employed for the selective absorption of saline water from various petroleum fraction–saline emulsions. Before these studies were begun, the swelling behavior of the Gg-cl-P(AAm-*co*-MAA) hydrogel polymer in various petroleum fractions, i.e., petrol, petroleum ether, kerosene and diesel, was examined. A 50 ml emulsion of each petroleum fraction (petrol, petroleum ether, kerosene and diesel) and saline water (1% NaCl solution) was prepared in a 1:1 v/v ratio and placed in a 250 ml conical flask. Each emulsion was stabilized by the addition of 10 ml of Tween-20, and the flasks were shaken in an automatic shaker machine (LABCO, India). After the formation of stable emulsions, 100 mg of hydrogel polymer was added to each emulsion and the flasks were shaken for an additional 20 h. After the completion of the experiment, the flasks were removed from the shaker and allowed to stand undisturbed for 48 h to break up the emulsions. After the breakup of the emulsions, the petroleum fractions and unabsorbed saline water were separated using a separating funnel, and the remaining, i.e., unabsorbed, volume of saline water was measured.

2.7. Flocculation studies

The flocculation studies of the Gg-cl-P(AAm-*co*-MAA) hydrogel polymer were conducted using the standard jar test (Jha, Agarwal, Mishra, & Rai, 2001). A 50 ppm kaolin solution was used as a clay suspension. A volume of 500 ml of this clay suspension was placed in a 1000 ml glass beaker and ultra-sonicated for 30 min, followed by vigorous stirring for 20 min at 250 rpm, for the complete dispersion of the clay particles. Afterward, a known amount of the already swollen hydrogel polymer was added to the clay suspension and agitated for 15 min at 200 rpm. At predefined time intervals, 5 ml sample aliquots were drawn and the turbidity was measured using a Micro 1000 IR Turbidimeter (HF Scientific Incorporation, USA). A control experiment was also performed in the absence of any hydrogel polymer to investigate the effects of the various experimental conditions (i.e., pH, concentration of suspended clay particles and temperature) on the natural decantation of the clay particles in the suspension. Various doses of the Gg-cl-P(AAm-*co*-MAA) hydrogel polymer were used to determine the maximum flocculation efficiency, followed by the evaluation of the maximum flocculation efficiency at varied temperatures and solution pH values.

2.8. Metal ion adsorption studies

The Gg-cl-P(AAm-*co*-MAA) hydrogel polymer was also utilized as an adsorbent for the removal of Pb^{2+} and Cu^{2+} metal ions from aqueous solutions. The adsorption of both metal ions was carried-out in batch mode. The pH value of both metal ion solutions was held equal to 5.0 to avoid the precipitation of the metal ions (Paulino et al., 2011). Initially, volumes of 50 ml of the metal-ion solutions (50 mg/l) were placed into individual plastic bottles. Various amounts of Gg-cl-P(AAm-*co*-MAA) hydrogel polymer were added to the metal ion solutions. The bottles were shaken in a thermostatic water bath shaker for 24 h at 200 rpm. After the completion of the experiment, the bottles were removed from the shaker, and the solutions were filtered using 0.45 μm cellulose acetate syringe filters. The concentration of metal ions remaining in each solution was measured using an atomic adsorption spectrophotometer (AAS). The adsorption efficiency or percentage removal was calculated by using the following equation:

$$\%\ \text{removal} = \frac{(C_o - C_e)}{C_o} \times 100 \quad (3)$$

where C_o is the initial concentration of metal ion and C_e is the equilibrium concentration of metal ion remained in the solution.

3. Results and discussion

3.1. Synthesis of the Gg-cl-P(AAm-co-MAA) hydrogel polymer

Cross linked hydrogel polymers of Gg with P(AAm-*co*-MAA) co-polymer were synthesized with five different concentrations of MAA in the range of 3.51 to 8.201 mol/l, whereas the concentration of AAm was held constant (i.e., 0.9859 mol/l) (Mittal et al., 2010). The selection of the optimal hydrogel polymer sample for the remaining studies was performed on the basis of the swelling capacity. The maximum swelling capacity was exhibited by the hydrogel polymer with a 4.68 mol/l concentration of MAA (Table S1, Supplementary information). P_s was found to increase with increasing MAA concentration until it reached a maximum of 1136%; then any further increase in monomer concentration resulted in a decrease in P_s. This phenomenon can be understood by considering that further increase in the MAA concentration beyond the optimum level resulted in an increased cross linking density,

producing a more compact hydrogel polymer with a lesser swelling capacity (Pourjavadi, Hosseinzadeh, & Mazidi, 2005).

3.1.1. Optimal mechanism

The best possible mechanism for the synthesis of a Gg-cl-P(AAm-*co*-MAA) hydrogel polymer using a mixture of ascorbic acid and KPS as a redox initiator and MBA as a cross linking agent in the microwave-assisted graft co-polymerization method is proposed in Scheme 1.

Initially, the ascorbic acid ions react with KPS and generate SO_4^{-*}, which, upon subsequent reactions with water molecules, generates OH^*; this is followed by the interaction of OH^* and SO_4^{-*} with Gg and monomers, which generates active sites for graft co-polymerization. Activated P(AAm-*co*-MAA) and Gg free radicals will further react and form a cross linked hydrogel polymer, using MBA as the cross linker to establish links between different polymeric chains. However, chain-termination reactions may occur, either through the reaction of OH^* with live propagating macromolecular chains or through reactions between two activated chains.

3.1.2. Thermogravimetric analysis, differential thermal analysis and differential thermo-gravimetric analysis (TGA/DTA/DTG)

The thermogram (i.e., TGA, DTA and DTG) of the Gg-cl-P(AAM-*co*-MAA) hydrogel polymer is presented in Fig. S2, Supplementary information. The initial decomposition temperature (IDT), final decomposition temperature (FDT) and decomposition temperatures per 10% weight loss are summarized in Table 1. Generally, the thermal decomposition of a polysaccharide involves the initial desorption of physically adsorbed water, dehydration reactions and subsequent depolymerization reactions, which include the rupture of C—O and C—C bonds in the rings and result in the evolution of CO, CO_2 and H_2O; then the final decomposition stage is characterized by the formation of polynuclear aromatic and graphitic carbon structures (Parikha & Madamwar, 2006).

In the case of Gg, decomposition occurs between 206.9 and 521.6 °C (Kaith, Jindal, Mittal, & Kumar, 2012a,b). Three-stages decomposition was observed from the TGA of Gg. These decomposition stages began at 206.9 °C (remaining residue = 84.01%), 331.4 °C (remaining residue = 37.3%) and 468.13 °C (remaining residue = 23.73%). The first stage of decomposition in Gg, which began at 206.9 °C may be associated both with dehydration reactions and some initial depolymerization reactions, as the maximum weight loss occurred in this stage of decomposition. The second stage of decomposition began at 331.4 °C. In this decomposition stage, the depolymerization reactions that began in the first stage most likely continued. The third and final stage of decomposition, which began at 468.13 °C, may have involved the formation of polynuclear aromatic and graphitic carbon structures (Singh, Sharma, & Pal, 2011).

The IDT and FDT of Gg were found to be 206.9 °C and 521.6 °C, respectively. By contrast, the decomposition of the Gg-cl-P(AAm-*co*-MAA) hydrogel polymer occurred between 148.0 and 552.6 °C (Fig. S2, Supplementary information). The TGA of the Gg-cl-P(AAm-*co*-MAA) hydrogel polymer also indicated three-stage decomposition; these stages began at 148 °C (remaining residue = 85.3%), 327.2 °C (remaining residue = 61%) and 441.5 °C (remaining residue = 20.6%). The first stage of decomposition, which occurred between 148.0 and 327.2 °C, may be associated with dehydration reactions. The second stage of decomposition involved both depolymerization reactions and the breaking of cross links between different polymeric chains between 327.2 and 441.5 °C, as the maximum weight loss (40.9%) was observed in this decomposition stage. The third and final stage of decomposition was observed between 441.5 and 552.6 °C. In this stage, the formation of polynuclear aromatic and graphitic carbon structures most likely took place. The Gg-cl-P(AAm-MAA) hydrogel polymer exhibited IDT and FDT values of 148.0 and 552.6 °C, respectively. The IDT of the Gg-cl-P(AAm-*co*-MAA) hydrogel polymer was found to be much lower than that of Gg, whereas the FDT of the hydrogen polymer was found to be much higher. The graft co-polymerization of Gg with P(AAm-*co*-MAA) may lower the IDT because of the decomposition of P(AAm-*co*-MAA) chains that accompanies the formation of imide groups and the evolution of ammonia (Behari, Pandey, Kumar, & Taunk, 2001). In turn, the formation of imide groups increases the FDT of the hydrogel polymer, thereby causing higher FDT to be observed in the case of the Gg-cl-P(AAm-*co*-MAA) hydrogel polymer than that observed for Gg. Furthermore, from the comparison of the decomposition temperatures per 10% weight loss, it is clear that the most marked weight loss occurred at higher temperatures for the Gg-cl-P(AAm-*co*-MAA) hydrogel polymer than for Gg (Table 1). From Table 1 it is also evident that almost 60% of the decomposition occurred at lower temperatures for the hydrogel polymer than for Gg, whereas beyond 60% decomposition, i.e., after the formation of imide groups, the decomposition occurred at higher temperatures in the hydrogel polymer. The DTA of Gg revealed two exothermic peaks at 483.2 °C (203 μV) and 492.7 °C (154 μV), thereby confirming the exothermic decomposition of Gg (Kaith et al., 2012a,b). By contrast, the DTA of the Gg-cl-P(AAm-*co*-MAA) hydrogel polymer revealed exothermic peaks at 496.6 °C (45.5 μV) and 553.3 °C (177.5 μV). Thus, the DTA decompositions were observed at higher temperatures in the case of the Gg-cl-P(AAm-*co*-MAA) hydrogel polymer than in the case of Gg. The DTG analyses of Gg and the Gg-cl-P(AAm-*co*-MAA) hydrogel polymer were performed to investigate the rate of mass loss (mg/min) versus temperature (°C). The DTG results for Gg indicated decompositions at 299.1 °C and 479.0 °C with mass-loss rates of 1.463 and 2.23 mg/min, respectively. However, the DTG results for the Gg-cl-P(AAm-*co*-MAA) hydrogel polymer indicated decompositions at 415.9 °C and 552.2 °C with mass-loss rates of 0.53 mg/min and 1.121 mg/min, respectively. From the DTG studies, it was observed that the hydrogel polymer exhibited DTG peaks at higher temperatures with lower rates mass-loss. Therefore, the above results clearly demonstrate that the Gg-cl-P(AAm-*co*-MAA) hydrogel polymer was more thermally stable compared with backbone polymer, i.e., Gg because of the formation of crosslinks between different polymeric chains through covalent bonding (Kaith et al., 2012a,b).

3.2. Swelling studies of the Gg-cl-P(AAm-co-MAA) hydrogel polymer in distilled water

Swelling in water is one of the most important and promising properties of hydrogel polymers. Most industrial applications of hydrogel polymers are associated with their ability to swell in water. Therefore, the swelling capacity of the Gg-cl-P(AAM-*co*-MAA) hydrogel polymer was investigated as a function of the swelling time, the temperature and the pH of the swelling medium.

The effect of the swelling time on P_s was studied at room temperature and neutral pH, and the weight of the swelled hydrogel polymer was determined at regular time intervals. It was observed that the percentage swelling increased with increasing swelling time and reached a maximum value of 1145% after 20 h (Fig. 1(a)). It is evident from Fig. 1(a) that after the maximum swelling capacity was attained, no further increase in P_s was observed with increasing in swelling time. This plateau behavior may be attributed to the porous structure of the hydrogel polymer becoming fully saturated at the point of maximum swelling, after which no space remained for the accommodation of more water molecules. After the optimization of the swelling time, the temperature of the swelling medium was optimized at the pre-optimized swelling time in a neutral medium. Initially, the percentage swelling increased with increasing temperature and

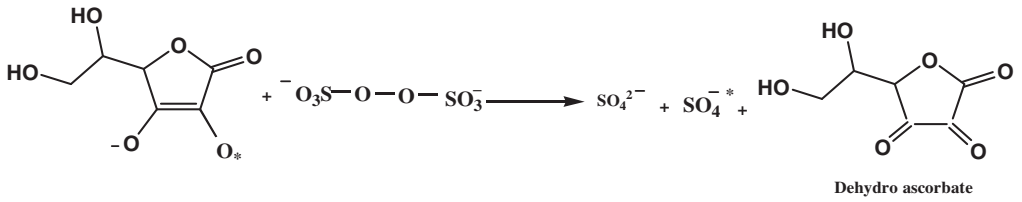

(1)

(2)

(3)

(4)

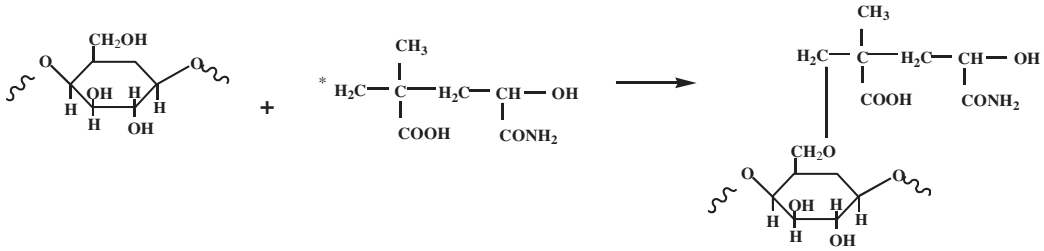

(5)

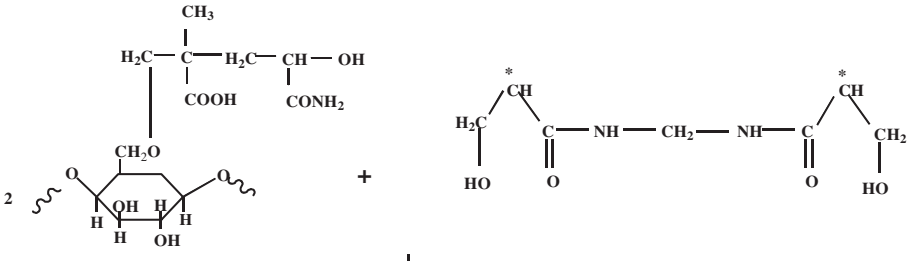

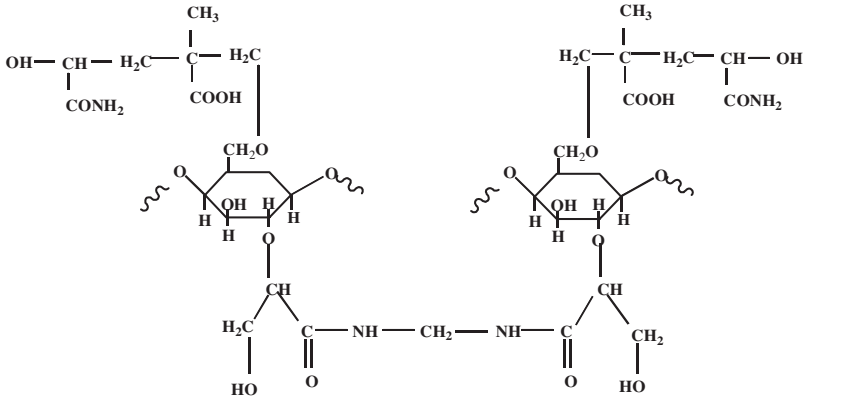

(7)

Scheme 1. Best possible proposed mechanism for the graft co-polymerization of Gg with P(AAm-*co*-MAA).

Table 1
Comparison of percentage thermal decompositions of Gg and Gg-cl-P(AAm-*co*-MAA) hydrogel polymer.

Sample code	Percentage decomposition at different temperatures (K)									
	IDT	20%	30%	40%	50%	60%	70%	80%	90%	FDT
Gg	273.15	233.67	255.45	277.34	296.83	318.05	394.32	483.44	490.09	521.6
Gg-cl-P(AAm-*co*-MAA)	148.0	193.41	245.71	333.39	367.74	394.26	415.51	444.93	521.22	552.6

Where IDT = initial decomposition temperature and FDT = final decomposition temperature.

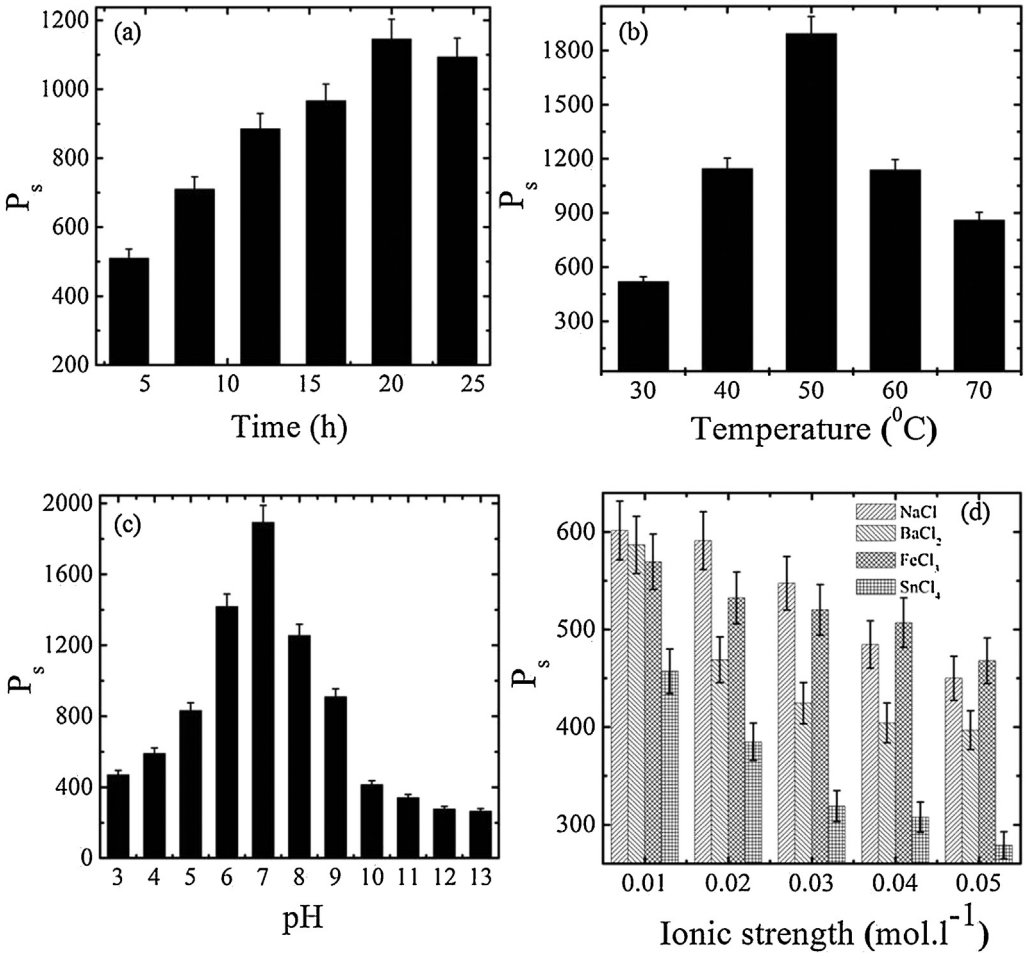

Fig. 1. ((a)–(d)) Effects of (a) time, (b) temperature, (c) pH and (d) ionic strength of different cations on the P_s of the Gg-cl-P(AAm-*co*-MAA) hydrogel polymer.

reached a maximum value of P_s (1959%) at 60 °C (Fig. 1(b)), whereas further increase in the temperature of the swelling medium P_s was caused to decrease. This behavior may be interpreted as follows: initially, an increase in the temperature caused the elasticity of the polymeric matrix to increase, which resulted in an increase in P_s; however, after the optimum temperature, leading to collapse with the further increase in temperature, leading to desorption. Moreover, hydrophilic groups of the hydrogels formed hydrogen bonds with water molecules. These bonds cooperatively formed a stable shell of hydration around the hydrophilic groups, leading to greater uptake of water and resulting in a greater P_s. However, the associated interactions among the hydrophilic groups caused the entrapped water molecules to be released from the hydrogel network at higher temperatures. Therefore, lower P_s was observed at higher temperatures (Feil, Bae, Feijen, & Kim, 1992; Inomato, Goto, & Saito, 1990).

The pH of the swelling medium was also found to have a profound effect on the swelling capacity of hydrogel polymer. A number of studies have been reported in the literature in which the effect of the solution pH on the swelling capacity of hydrogel polymers has been investigated (Inomato et al., 1990; Kaith et al., 2012a,b; Singh et al., 2011). The effect of the solution pH on the P_s of the Gg-cl-P(AAm-*co*-MAA) hydrogel polymer was studied in solutions of various pH values in the range of 3.0 to 13.0 at the pre-optimized swelling time and the pre-optimized temperature of the swelling medium. Fig. 1(c) shows the effect of the solution pH on the swelling capacity of the hydrogel polymer. From this figure, it is apparent that the Gg-cl-P(AAm-*co*-MAA) hydrogel polymer exhibited the maximum swelling capacity (1959%) in a neutral medium and lesser swelling capacities in alkaline and acidic media. Initially, P_s was found to increase as the solution pH changed from acidic to neutral, whereas a decline in P_s was again observed as the solution pH changed from neutral to alkaline. This type of swelling behavior as a function of the solution pH may be explained on the basis of osmotic swelling pressure (π_{ion}) theory. According to this theory, in dilute polyelectrolyte solutions, hydrogel polymers swell because of the swelling osmotic pressure between the gel phase and the external solution, and the extent of swelling depends on the

difference between the concentrations of mobile ions in the swollen gel (C_i^g) and in the external solutions (C_i^s) and is given by the following equation (Bajpai, 1999):

$$\pi_{ion} = RT \sum \left(C_i^g - C_i^s\right) \quad (4)$$

where (C_i^g) and (C_i^s) are the molar concentrations of mobile ions in the swollen gel and in the external solution, respectively. R is the gas constant and T is the absolute temperature.

In a neutral medium, the value of π_{ion} becomes very large because the concentration of mobile ions in the external solution (C_i^s) is almost negligible. Moreover, the electrostatic repulsion between carboxylate ions promotes swelling. However, in an acidic medium, most of the carboxylate and hydroxyl ions present in the hydrogel polymer network are protonated, leading to a decreased concentration of ions within the swollen gel (C_i^g); as a result, π_{ion} becomes small. On the other hand, in an alkaline solution, —COOH groups completely dissociate, but the concentrations of Na^+ and —OH ions are also very high, causing the values of π_{ion} and P_s to decrease. Moreover, in an alkaline medium, the screening effect of the counter ions (Na^+), shields the electrostatic repulsion between carboxylate anions; as a result, a remarkable decrease in P_s is observed (Kaith et al., 2012a,b).

The effect of the ionic strength and charge of the metal cations in the external solution on the swelling capacity of the Gg-cl-P(AAm-*co*-MAA) hydrogel polymer were also studied (Fig. 1(d)). The swelling capacity of the hydrogel polymer was found to decrease with increasing ionic strength of the metal cations. This decrease in P_s with increased ionic strength may be attributed to the fact that an increased molar concentration of cations in the external solutions causes the number of free ions in the external solution to increase, thereby reducing the osmotic swelling pressure and, therefore, the swelling capacity of the hydrogel polymer. Furthermore, the swelling capacity was also found to decrease for metal cations of higher charge ($Na^+ > Ba^{2+} > Fe^{3+} > Sn^{4+}$). Although the hydrogel polymer initially exhibited similar swelling behavior in each salt solution, after a certain time interval, a clear difference in the swelling behavior of the hydrogel polymer in the different salt solutions was observed. This difference may be attributed to the fact that for a higher cationic charge, the concentration of free mobile ions in the gel (C_i^g) will be lower, leading to the reduction of $\pi_{ion\ s}$ and P_s. Moreover, the ability of the carboxylate groups of the hydrogel to form complexes with multivalent cations will also lead to the reduction in P_s (Kaith, Ranjta, & Kumar, 2008; Kaith et al., 2012a,b).

3.3. Selective absorption of saline from various petroleum fraction–saline emulsions

The separation of saline water from crude petroleum during the extraction of petroleum products from sea water is a crucial concern. Hydrogel polymers have previously demonstrated some potential for use in the removal of saline water from various petroleum fraction–saline water emulsions (Kaith et al., 2012a,b; Mittal et al., 2013a). Therefore, in view of this unique property of hydrogel polymers, the Gg-cl-P(AAm-*co*-MAA) hydrogel polymer was utilized for the removal of saline water from various petroleum fraction–saline water emulsions, i.e., petroleum ether–saline water, petrol–saline water, diesel–saline water and kerosene–saline water emulsions. Before these experiments were began, the swelling behavior of the Gg-cl-P(AAm-*co*-MAA) hydrogel polymer was investigated in the various petroleum fractions that were studied, i.e., petrol, kerosene, diesel and petroleum ether. The Gg-cl-P(AAm-*co*-MAA) hydrogel polymer did not exhibit any swelling in any of the above mentioned petroleum fractions. The hydrogel polymer was found to absorb 46% of the saline water from the petroleum ether–saline emulsion, 40.5% of the saline water from the petrol–saline emulsion, 36.6% of the saline water from the kerosene–saline emulsion and 38.9% of the saline water from the diesel–saline emulsion (Table 2).

3.4. Flocculation properties of the Gg-cl-P(AAm-co-MAA) hydrogel polymer

3.4.1. Effect of polymer dose on flocculation efficiency

Fig. 2(a) shows the effect of the polymer dose on the flocculation efficiency of the Gg-cl-P(AAm-*co*-MAA) hydrogel polymer in a clay suspension of 50 mg/l. The flocculation efficiency of any polymer is strongly influenced by the dose of polymer that is added to the suspension. Generally, the flocculation efficiency decreases at higher or lower polymer doses than the optimum one (Ghimici et al., 2012). Flocculation efficiency is expressed in terms of the residual turbidity of the supernatant liquid. The lower the residual turbidity is, the better the flocculation efficiency will be. To investigate the effect of the polymer dose on the residual turbidity of the supernatant liquid, various amounts of hydrogel polymer (10, 15, 20 and 25 mg) were added to the clay suspension. Initially, the residual turbidity of the clay suspension was found to decrease with increasing polymer dose until the minimum value was attained; further increase in the polymer dose then caused the residual turbidity to increase once again. This behavior can be explained on the basis of the formation of a particle–polymer–particle complex, in which tails and loops of certain polymers with high affinity for the suspended particles in the supernatant liquid form bridges between two or more particles. Graft co-polymers have mostly been observed to follow this bridging mechanism in the flocculation process (Ghimici & Nichifor, 2010, 2012; Ghimici et al., 2012; Mittal et al., 2013b).

The Gg-cl-P(AAm-*co*-MAA) hydrogel polymer served to bridge two or more clay particles in the suspension. As soon as the clay particles came in contact with the hydrogel polymer, they became attached to various functional groups present in the polymer chains, leading to the formation of extended polymer chains. Furthermore, when other clay particles came in contact with one of these extended polymer chains; they also became attached to the other side of the polymer chain and formed a complex in which the hydrogel polymer acted as a bridge between different clay particles present in the supernatant liquid. Therefore, the residual turbidity was found to initially decrease with increasing polymer dose until minimum value was attained. At lower polymer doses, there were insufficient functional groups to act as bridges between different clay particles, whereas at higher polymer doses, the increased number of functional groups provided more bridges for the formation of particle–polymer–particle complexes, causing the residual turbidity to decrease. On the other hand, the residual turbidity of the clay suspension increased when the polymer dose was further increased beyond the optimum value because at doses above the optimum polymer dose, kaolin particles became enveloped between cross linked polymer chains and were not able to come into contact with the functional groups present on the polymer chains (Xie, Feng, Cao, Xia, & Lu, 2007). Therefore, the clay particles in the supernatant liquid re-stabilized, leading to a higher of turbidity.

3.4.2. Effect of temperature on flocculation efficiency

Fig. 2(b) shows the effect of the temperature on the flocculation efficiency of the Gg-cl-P(AAm-*co*-MAA) hydrogel polymer. The residual turbidity was found to initially decrease with increasing temperature, and a minimum turbidity of 1126.45 NTU was observed at 40 °C, as the temperature was further increased beyond this optimum value, the residual turbidity of the supernatant liquid again increased. Initially, the formation of particle–polymer–particle complexes was facilitated by the

Table 2
Percentage removal of saline from different petroleum fraction–saline emulsions.

Sample	Percentage saline removal											
	Kerosene–saline			Diesel–saline			Petrol–saline			Pet. ether–saline		
	% Removal	±SD	±SE	% Removal	±SD	±SE	% removal	±SD	±SE	% removal	±SD	±SE
Gg-cl-P(AAm-*co*-MAA)	40.5	1.45	0.83	43.5	0.87	0.50	36.5	1.53	0.88	46.0	1.31	0.75

Whereas, amount of each emulsion taken = 100 ml (1:1 v/v); weight of superabsorbent taken for each emulsion = 1.0 g.

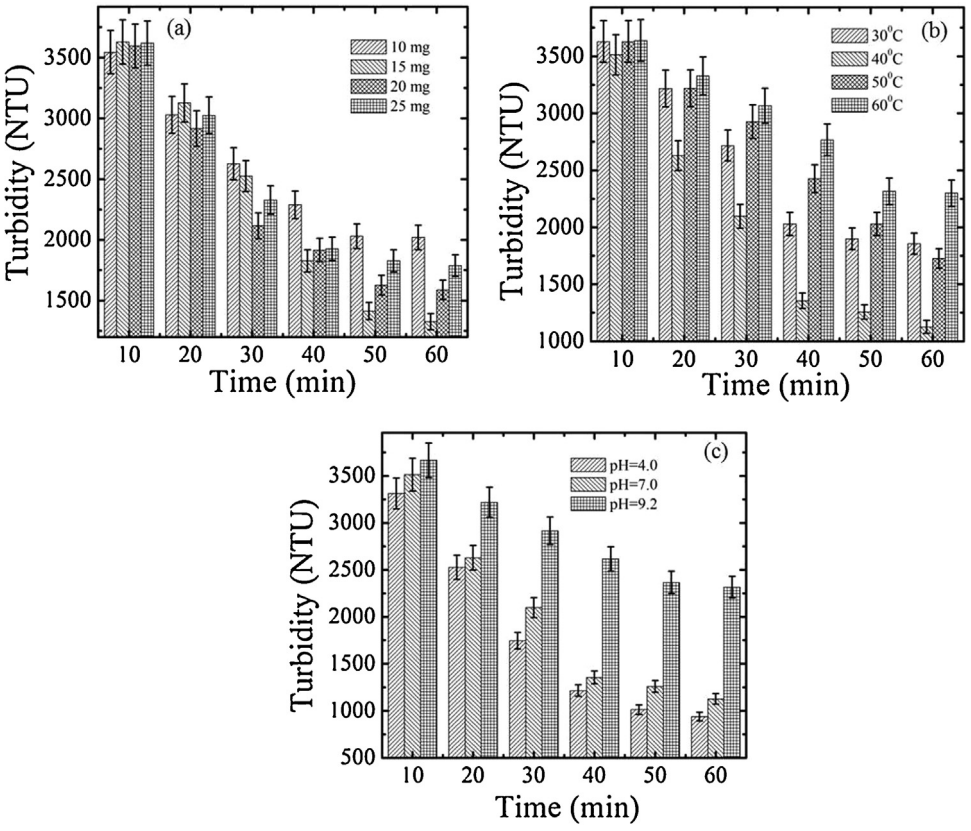

Fig. 2. ((a)–(c)) Effects of (a) time, (b) temperature and (c) pH on turbidity.

increase in temperature; however, after the minimum residual turbidity was reached, any further increase in temperature caused the kinetic energies of the hydrogel polymer molecules to increase, resulting in the re-dispersion of the kaolin particles and an increased residual turbidity (Mittal et al., 2013b).

3.4.3. *Effect of pH on flocculation efficiency*

Solution pH is a very important factor in flocculation because it affects the nature of the functional groups present on the polymer. The effect of the pH on the residual turbidity of the clay suspensions was examined at the pre-optimized polymer dose and temperature in suspensions of various pH values (4.0, 7.0 and 9.0). Fig. 2(c) presents the effect of the solution pH on the flocculation efficiency of the Gg-cl-P(AAm-*co*-MAA) hydrogel polymer. The acidic clay suspension was found to exhibit lower residual turbidity compared with the alkaline and neutral suspensions. This behavior may be attributed to the fact that in an acidic pH solution, the hydroxyl and acidic groups present in the hydrogel polymer are protonated, conferring overall cationic charge to the hydrogel polymer; therefore the negatively charged clay particles readily attach to these cationic functional groups to form particle–polymer–particle complexes, thereby reducing the residual turbidity of the clay suspension (Mittal et al., 2013b). However, in an alkaline medium, the protonation of the hydroxyl and carboxylate ions is not possible, so the formation of particle–polymer particle complexes do not occur because of the anionic-anionic repulsion between the functional groups of the hydrogel polymer and the negatively charged particles in the clay suspension; therefore, comparatively a higher residual turbidity was observed in the alkaline clay suspension. The probable mechanism of the flocculation behavior of the Gg-cl-P(AAm-*co*-MAA) hydrogel polymer at various solution pH is shown in Fig. S3 (Supplementary information).

3.5. *Biodegradation studies of the Gg-cl-P(AAm-co-MAA) hydrogel polymer*

The ability of gum-polysaccharide-based hydrogels to degrade under both aerobic and anaerobic conditions is one of their remarkable properties. Gum polysaccharides have typically been modified with synthetic monomers to improve their properties for various industrial applications. However, during the modification process, care must be taken that the biodegradable nature of the gum polysaccharide is not affected. The biodegradable nature of Gg-based graft co-polymers has already been demonstrated (Mittal et al., 2013b; Sharma et al., 2014). The biodegradable nature of the cross linked graft co-polymer synthesized in this study,

Table 3
Biodegradation studies of Gg-cl-P(AAm-*co*-MAA) hydrogel polymer using composting method.

Sample code	Percentage weight loss at different time intervals (days)									
	5	10	15	20	25	30	35	40	45	50
Gg	43.24	73.09	93.78	100	–	–	–	–	–	–
Gg-cl-poly(AAm-*co*-MAA)	17.85	30.00	36.58	57.33	66.86	82.10	88.37	89.79	95.45	100.00

i.e., the Gg-cl-P(AAm-*co*-MAA) hydrogel polymer, was examined using the soil composting method. In case of bio-based polymers, the process of biodegradation typically begins with the backbone polymer, i.e., the biopolymer. Therefore, in this case, the degradation process began with Gg. It was observed that the weight of the hydrogel polymer decreased continuously and that the rate of weight loss was lower in the initial stages than in the later stages of biodegradation. The slow rate of degradation in the initial stages of biodegradation may be attributable to the fact that the hydrogel polymer initially absorbs some water, leading to a lower overall rate of weight loss. After some time, however, under the action of the microbes present in the soil compost, the hydrogel polymer begins to collapse under the weight of the absorbed water and begins to degrade much more rapidly. The Gg-cl-P(AAm-*co*-MAA) hydrogel polymer was found to degrade completely within 50 days (Table 3). The various processes involved in the degradation of the hydrogel polymer included enzymatic and chemical degradation. The secretion products of the microbes present in the composting media were also involved in the degradation of the hydrogel polymer samples and caused the cleavage of chemical bonds and bacterial degradation (Kaith, Jindal, Maiti, & Jana, 2010).

3.5.1. Evidence of bio-degradation

3.5.1.1. Spectroscopic studies. The graft co-polymerization of Gg with the co-polymeric mixture of P(AAm-*co*-MAA) as well as the degradation of the Gg-cl-P(AAm-*co*-MAA) hydrogel polymer were confirmed through FTIR analyses. The FTIR spectra of the Gg-cl-P(AAm-*co*-MAA) hydrogel polymer before the initialization of the graft co-polymerization reaction and at various stages of biodegradation are presented in Fig. 3. The FTIR spectrum of the Gg-cl-P(AAm-*co*-MAA) hydrogel polymer exhibited peaks at 1711.23 cm^{-1} (C=O stretching of MAA), 1619.23 cm^{-1} (C=O stretching of amide-I), 1395.97 cm^{-1} (NH in plane bending of amide-II) and 1237.45 cm^{-1} (CN stretching of amide-III) (Fig. 3(a)) in addition to with the peaks observed in the FTIR spectrum of Gg (Kaith et al., 2012a,b). The presence of these peaks in the FTIR spectrum of the cross linked hydrogel polymer confirmed the successful graft co-polymerization of Gg with the co-polymer mixture of P(AAm-*co*-MAA).

The FTIR spectra of the hydrogel polymer at various stages of biodegradation exhibited variations in the positions of certain peaks and the reductions of the intensity of certain other peaks. In the FTIR spectrum of the sample at stage-I biodegradation, the peaks that were initially observed at 1619.23 and 1711.23 cm^{-1} were found to be shifted (Fig. 3(b)) and reduced in intensity, confirming the onset of the biodegradation process. The shifting of the peaks observed in the first stage of biodegradation may be attributed to the breakage of cross links between different polymeric chains caused by the secreted products of micro-organisms; these secreted products caused most bonds break and yield various by-products, resulting in the appearance of new peaks in addition to the shifting of peaks already present in the FTIR spectrum. In the second stage of biodegradation, the disintegration and degradation of individual compounds of the Gg-cl-P(AAm-*co*-MAA) hydrogel polymer began (Fig. 3(c)). In the FTIR spectrum of the hydrogel polymer of at stage-II biodegradation, the peaks associated with Gg and the binary monomers disappeared because of the cleavage of the P(AAm-*co*-MAA) chains from the backbone polymer. In the third and final stage of biodegradation, most of the peaks that were initially observed in the FTIR spectrum of the Gg-cl-P(AAm-*co*-MAA) hydrogel polymer were found to have shifted or completely disappeared (Fig. 3(d)); this finding may be attributed to the complete breakdown of the polymer structure (Mittal et al., 2013b; Sharma et al., 2014). Thus, it is evident from the FTIR studies that the Gg-cl-P(AAm-*co*-MAA) hydrogel polymer was completely degraded in the soil compost within a period of 50 days.

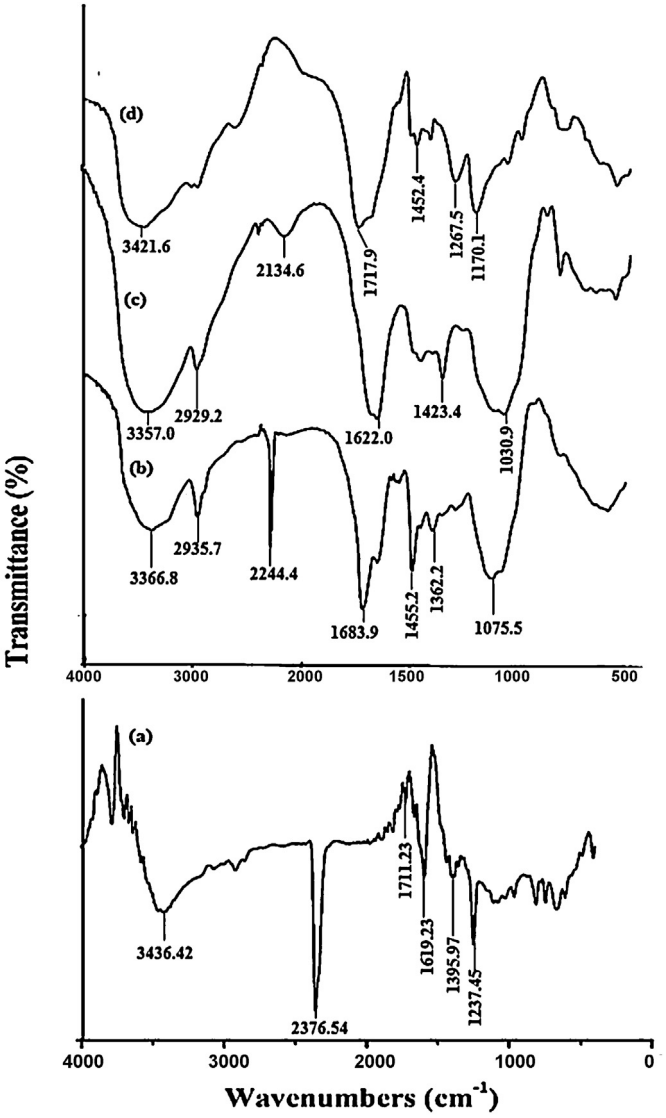

Fig. 3. ((a)–(d)) FTIR spectra of (a) the Gg-cl-P(AAm-*co*-MAA) hydrogel polymer and (b) the Gg-cl-P(AAm-*co*-MAA) hydrogen polymer in stage-I of biodegradation and (c) the Gg-cl-P(AAm-*co*-MAA) hydrogen polymer in stage-II of biodegradation and (d) the Gg-cl-P(AAm-*co*-MAA) hydrogen polymer in stage-III of biodegradation.

3.5.1.2. Morphological studies. The changes in the morphology of the Gg-cl-P(AAm-*co*-MAA) hydrogel polymer after graft co-polymerization and at various stages of biodegradation were

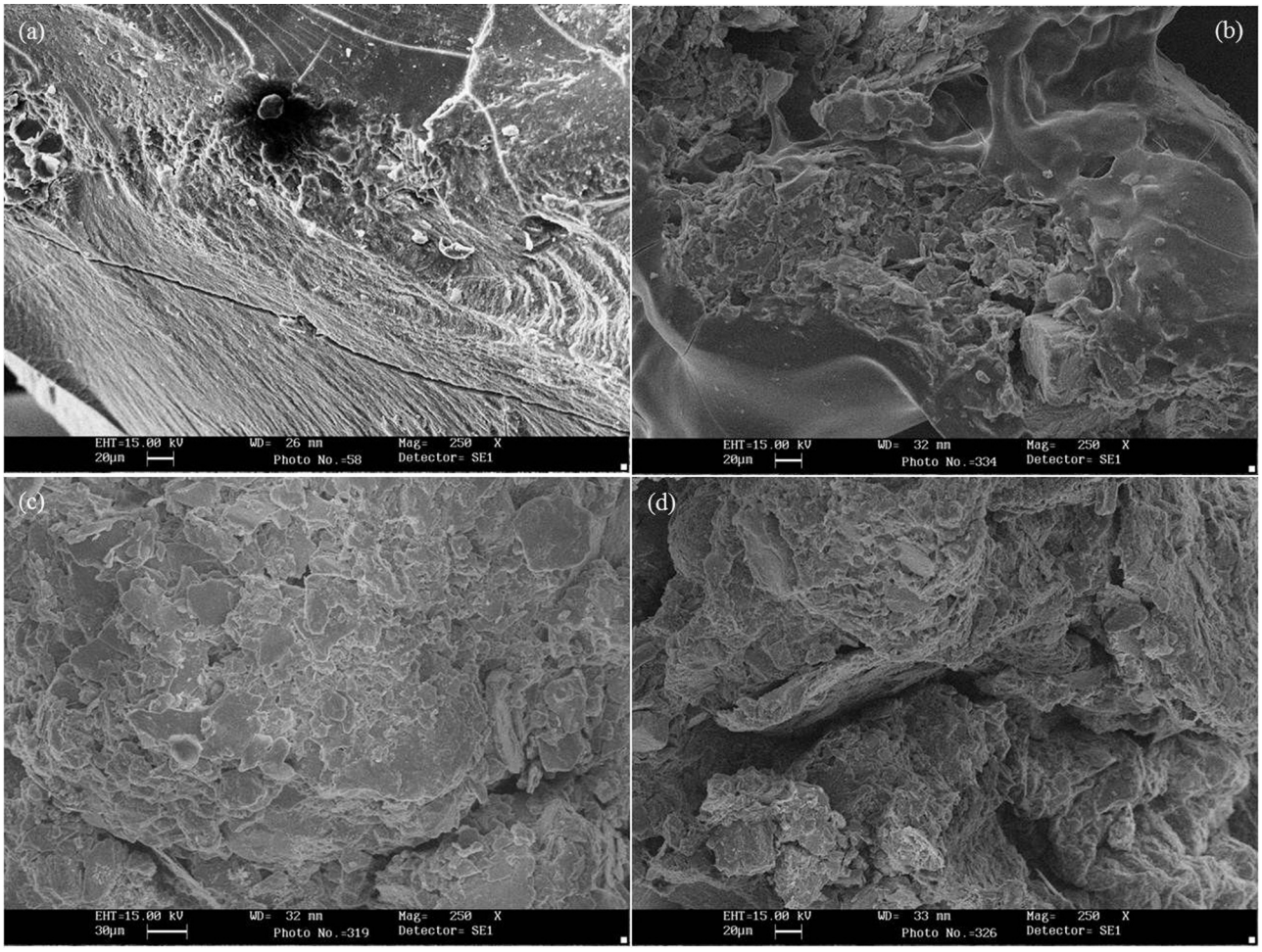

Fig. 4. ((a)–(d)) SEM images of (a) the Gg-cl-P(AAm-*co*-MAA) hydrogel polymer and (b) the Gg-cl-P(AAm-*co*-MAA) hydrogen polymer in stage-I of biodegradation and (c) the Gg-cl-P(AAm-*co*-MAA) hydrogen polymer in stage-II of biodegradation and (d) the Gg-cl-P(AAm-*co*-MAA) hydrogen polymer in stage-III of biodegradation.

studied by means of SEM. The surface of the Gg-cl-P(AAm-*co*-MAA) hydrogel polymer was found to be smooth and free of cracks with a continuous and regular morphology (Fig. 4(a)). By contrast, after biodegradation, the smooth surface of the hydrogel polymer became heterogeneous and full of cracks. The continuous morphology of the hydrogel polymer converted into a fibrilar one. In stage-I of biodegradation, some cracks, fractures and fissures began to appear on the surface of the Gg-cl-P(AAm-*co*-MAA) hydrogel polymer, indicating the onset of the biodegradation process and the breakdown of the polymer chains (Fig. 4(b)). In stage-II of biodegradation, the number and size of these fractures and fissures increased, confirming the progression of the biodegradation process (Fig. 4(c)). These larger cracks, fractures and fissures may have arisen because of the disintegration of individual compounds of the hydrogel polymer. In the third and final stage of biodegradation, i.e., stage-III, a drastic change in the surface morphology of the hydrogel polymer was observed. The initially homogeneous and continuous surface of the hydrogel polymer was completely converted into a heterogeneous and rough surface with many large cracks, fractures and fissures (Fig. 4(d)). This morphological change may be attributed to complete fracture of the cross linked network of the hydrogel polymer and the breakage of the covalent bonds between different polymer chains as a result of microbial activity (Mittal et al., 2013b; Sharma et al., 2014). Thus, it can be concluded from the SEM studies that the Gg-cl-P(AAm-*co*-MAA) hydrogel polymer was fully degraded when subjected to biodegradation using the soil composting method.

3.6. Adsorption of cationic dyes from aqueous solutions

The Gg-cl-P(AAm-*co*-MAA) hydrogel polymer was also utilized for the removal of toxic Pb^{2+} and Cu^{2+} metal ions from aqueous solutions (Fig. 5). The effect of polymer dose on the percentage adsorption of the metal ions was examined at various polymer doses varied from 5 to 40 mg. At the beginning, it was observed that the metal ions uptake increased with increasing polymer dose until the maximum percent adsorption was reached. The Gg-cl-P(AAm-*co*-MAA) hydrogel polymer was found to adsorb 94% of Pb^{2+} and 75% of Cu^{2+} from the corresponding salt solutions at polymer doses of with 20 and 30 mg, respectively. This increase in the percentage adsorption was due to the availability of more adsorption sites and increased surface area with increasing adsorbent dose.

On the other hand, no noticeable increase in the percentage adsorption was observed with further increase in the dose of adsorbent. This was due to the fact that after maximum adsorption the concentration of metal ions became limiting in the system. Moreover, the percentage adsorption of the metal ions did not increase with further increase in adsorbent dose because the total available surface area decreased due to the aggregation of the adsorption sites and the increased diffusion path length (Ghorai et al., 2014).

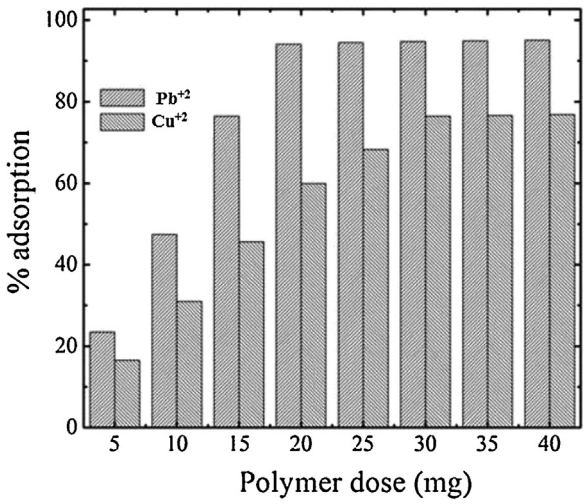

Fig. 5. Adsorption of Pb^{2+} and Cu^{2+} using the Gg-cl-P(AAm-*co*-MAA) hydrogel polymer.

The high adsorption of both the metal ions on the surface of the Gg-cl-P(AAm-*co*-MAA) hydrogel polymer is due to the presence of anionic binding sites on the surface of gum polysaccharides; therefore, there was an electrostatic attraction between the negatively charged functional groups on the surface of the Gg-cl-P(AAm-*co*-MAA) hydrogel polymer and the cationic metal ions, and the metal ions could very easily attach to the negative binding sites of the hydrogel polymer.

4. Conclusions

A biodegradable flocculent based on a hydrogel polymer of Gg with a co-polymer mixture of P(AAm-*co*-MAA) was successfully synthesized using a microwave-assisted technique. The thermal stability of the hydrogel polymer was much higher than that of Gg. The Gg-cl-P(AAm-*co*-MAA) hydrogel polymer demonstrated an excellent swelling capacity in distilled water and swelled by up to 1959% at 60 °C. It was found that the swelling capacity of the hydrogel polymer could be effectively reduced by adjusting the ionic strength and cationic change of the external solution. The hydrogel polymer absorbed saline water from various petroleum fraction saline emulsions. The Gg-cl-P(AAm-*co*-MAA) hydrogel polymer exhibited its maximum flocculation efficiency in acidic pH conditions at a 15 mg hydrogel polymer dose. Furthermore, the graft co-polymerization reaction did not affect the biodegradable nature of the hydrogel polymer. The Gg-cl-P(AAm-*co*-MAA) hydrogel polymer was found to degrade completely within 50 days of biodegradation. The hydrogel polymer was also utilized as an effective adsorbent for the adsorption of Pb^{2+} and Cu^{2+} from aqueous solutions. Therefore, from these studies, it can be concluded that the cross linked hydrogel polymer of Gg with P(AAm-*co*-MAA) that was synthesized using the microwave-assisted graft co-polymerization technique is fully biodegradable and appropriate for use in industrial waste-water treatment. In future, we will conduct our field study of such an application of the polymer.

Acknowledgement

The authors are grateful to the National Research Foundation (NRF), South Africa for awarding a Postdoctoral research fellowship to Dr. Hemant Mittal. The authors (HM, AM, SSR) would also like to thank the Department of Science and Technology and the Council for Scientific and Industrial Research, South Africa for their financial support.

Appendix A. Supplementary data

Supplementary data associated with this article can be found, in the online version, at http://dx.doi.org/10.1016/j.carbpol.2014.09.026.

References

Alvarez-Manceñido, F., Landin, M., Lacik, I., & Martínez-Pacheco, R. (2008). Konjac glucomannan and konjac glucomannan/xanthan gum mixtures as excipients for controlled drug delivery systems. Diffusion of small drugs. *International Journal of Pharmaceutics*, *349*, 11–18.

Ashori, A. (2008). Wood-plastic composites as ptomising green-composites for automotive industries. *Bioresource Technology*, *99*, 4661–4667.

Aspinall, G. O., Hirst, E. L., & Wickstrom, A. (1955). Gum ghatti (Indian gum). The composition of the gum and the structure of two aldobiouronic acids derived from it. *Journal of the Chemical Society*, 1160–1165.

Aspinall, G. O. (1980). Chemistry of cell wall polysaccharides. In J. Preiss (Ed.), *The biochemistry of plants* (pp. 473–500). New York, NY: Academic Press.

Bajpai, S. K. (1999). Casein crosslinked polyacrylamide hydrogels: Study of swelling and drug release behaviour. *Iranian Polymer Journal*, *8*, 231–239.

Behari, K., Pandey, P. K., Kumar, R., & Taunk, K. (2001). Graft copolymerization of acrylamide onto xanthan gum. *Carbohydrate Polymers*, *46*, 185–189.

Feil, H., Bae, Y. H., Feijen, J., & Kim, S. W. (1992). Mutual influence of pH and temperature on the swelling of ionizable and thermosensitive hydrogels. *Macromolecules*, *25*, 5528–5530.

Gaudreault, R. N., Cesare, N. D., Weitz, D., & van de Ven, T. G. M. (2009). Flocculation kinetics of precipitated calcium carbonate. *Colloids and Surfaces A: Physicochemical and Engineering Aspects*, *340*, 56–65.

Ghimici, L., & Nichifor, M. (2010). Novel biodegradable flocculanting agents based on cationic amphiphilic polysaccharides. *Bioresource Technology*, *101*, 8549–8554.

Ghimici, L., & Nichifor, M. (2012). Flocculation by cationic amphiphilic polyelectrolyte: Relating efficiency with the association of polyelectrolyte in the initial solution. *Colloids and Surfaces A: Physicochemical and Engineering Aspects*, *415*, 142–147.

Ghimici, L., Constantin, M., & Fundueanu, G. (2012). Novel biodegradable flocculanting agents based on pullulan. *Journal of Hazardous Materials*, *181*, 351–358.

Ghorai, S., Sarkar, A., Raoufi, M., Panda, A. B., Schönherr, H., & Pal, S. (2014). Enhanced removal of methylene blue and methyl violet dyes from aqueous solution using a nanocomposite of hydrolyzed polyacrylamide grafted xanthan gum and incorporated nanosilica. *ACS Applied Materials and Interfaces*, *6*, 4766–4777.

Guo, J., Ge, L., Li, X., Mu, C., & Li, D. (2014). Periodate oxidation of xanthan gum and its crosslinking effects on gelatin-based edible films. *Food Hydrocolloids*, *39*, 243–250.

Ho, I. C., Norli, I., Alkarkhi, A. F. M., & Morad, N. (2010). Characterization of biopolymeric flocculant (pectin) and organic synthetic flocculant (PAM): A comparative study on treatment and optimization in kaolin suspension. *Bioresource Technology*, *101*, 1166–1174.

Inomato, H., Goto, S., & Saito, S. (1990). Phase transition of N-substituted acrylamide gels. *Macromolecules*, *23*, 4887–4888.

Jha, A., Agarwal, S., Mishra, A., & Rai, J. S. P. (2001). Synthesis, characterization and flocculation efficiency of poly(acrylamide-*co*-acrylic acid) in tanne. *Iranian Polymer Journal*, *10*, 85–90.

Kaith, B. S., Ranjta, S., & Kumar, K. (2008). In-air synthesis of GA-cl-poly(MAA) hydrogel and study of its salt-resistant swelling behavior in different salts. *e-Polymers*, 158 (no.)

Kaith, B. S., Jindal, R., Maiti, M., & Jana, A. K. (2010). Development of corn starch based green composites reinforced with *Saccharum spontaneum* L. fiber and graft copolymers—Evaluation of thermal, physico-chemical and mechanical properties. *Bioresource Technology*, *101*, 6843–6851.

Kaith, B. S., Jindal, R., Mittal, H., & Kumar, K. (2012a). Synthesis, characterization and swelling behavior evaluation of Gum ghatti and acrylamide based hydrogel for selective absorption of saline from different petroleum fraction–saline emulsions. *Journal of Applied Polymer Science*, *124*, 2037–2047.

Kaith, B. S., Jindal, R., Mittal, H., & Kumar, K. (2012b). Synthesis of crosslinked networks of Gum ghatti with different vinyl monomer mixtures and effect of ionic strength of various cations on its swelling behavior. *International Journal of Polymeric Materials*, *61*, 99–115.

Malik, S., Kumar, A., & Ahuja, M. (2012). Synthesis of gum kondagogu-*g*-poly(*N*-vinyl-2-pyrrolidone) and its evaluation as a mucoadhesive polymer. *International Journal of Biological Macromolecules*, *51*, 56–62.

Mishra, M. M., Sand, A., Mishra, D. K., Yadav, M., & Behari, K. (2010). Free radical graft copolymerization of *N*-vinyl-2-pyrrolidone onto k-carrageenan in aqueous media and applications. *Carbohydrate Polymers*, *82*, 424–431.

Mittal, H., Kaith, B. S., & Jindal, R. (2010). Microwave radiation induced synthesis of Gum ghatti and acrylamide based crosslinked network and evaluation of its thermal and electrical behavior. *Der Chemica Sinica*, *1*, 59–69.

Mittal, H., Fosso-Kankeu, E., Mishra, S., & Mishra, A. (2013). Biosorption potential of Gum ghatti-*g*-poly(acrylic acid) and susceptibility to biodegradation by *B. subtilis*. *International Journal of Biological Macromolecules*, *62*, 370–378.

Mittal, H., Mishra, S. B., Mishra, A. K., Kaith, B. S., & Jindal, R. (2013). Flocculation characteristics and biodegradation studies of Gum ghatti based hydrogels. *International Journal of Biological Macromolecules*, *58*, 37–46.

Mittal, H., Ballav, N., & Mishra, S. (2014). Gum ghatti and Fe_3O_4 magnetic nanoparticles based nanocomposites for the effective adsorption of methylene blue from aqueous solution. *Journal of Industrial and Engineering Chemistry*, *20*, 2184–2192.

Mittal, H., & Mishra, S. (2014). Gum ghatti and Fe_3O_4 magnetic nanoparticles based nanocomposites for the effective adsorption of Rhodamine B. *Carbohydrate Polymers*, *101*, 1255–1264.

Nayak, P. L. (2000). Natural oil based polymers: Opportunities and challenges. *Journal of Macromolecular Science—Reviews in Macromolecular Chemistry and Physics*, *40*, 1–21.

Parikha, A., & Madamwar, D. (2006). Partial characterization of extracellular polysaccharides from cyanobacteria. *Bioresource Technology*, *97*, 1822–1827.

Paulino, A. T., Belfiore, L. A., Kubota, L. T., Muniz, E. C., Almeida, V. C., & Tambourgi, E. B. (2011). Effect of magnetite on the adsorption behavior of Pb(II), Cd(II), and Cu(II) in chitosan-based hydrogels. *Desalination*, *275*, 187–196.

Pourjavadi, A., Hosseinzadeh, H., & Mazidi, R. (2005). Modified carrageenan. 4. Synthesis and behaviour of crosslinked kC-g-AMPS superabsorbent hydrogel with anti-salt and pH-responsiveness properties. *Journal of Applied Polymer Science*, *98*, 255–263.

Rani, P., Sen, G., Mishra, S., & Jha, U. (2010). Microwave assisted synthesis of polyacrylamide grafted gum ghatti and its application as flocculant. *Carbohydrate Polymers*, *89*, 275–281.

Raul Muñoz, R., & Benoit Guieysse, B. (2006). Algal-bacterial processes for the treatment of hazardous contaminants: A review. *Water Research*, *40*, 2799–2815.

Sand, A., Yadav, M., Mishra, M. M., Tripathy, J., & Behari, K. (2011). Studies on graft copolymerization of 2-acrylamidoglycolic acid on to partially carboxymethylated guar gum and physico-chemical properties. *Carbohydrate Polymers*, *83*, 14–21.

Sharma, K., Kaith, B. S., Kumar, V., Kalia, S., Kumar, V., & Swart, H. C. (2014). Synthesis and biodegradation studies of gamma irradiated electrically conductive hydrogels. *Polymer Degradation & Stability*, *107*, 166–177.

Shi, H.-Y., & Zhang, L.-M. (2007). New grafted polysaccharides based on *O*-carboxymethyl-*O*-hydroxypropyl guar gum and *N*-isopropylacrylamide: Synthesis and phase transition. *Carbohydrate Polymers*, *67*, 337–342.

Shi, X.-N., Wang, W. B., & Wang, A. Q. (2011). Effect of surfactant on porosity and swelling behaviors of guar gum-g-poly(sodium acrylate-*co*-styrene)/attapulgite superabsorbent hydrogels. *Colloids and Surfaces B: Biointerfaces*, *88*, 279–286.

Singh, B., Sharma, V., & Pal, L. (2011). Formation of sterculia polysaccharide networks by gamma rays induced graft copolymerization for biomedical applications. *Carbohydrate Polymers*, *86*, 1371–1380.

Singh, R. P., Tripathy, T., Karmakar, G. P., Rath, S. K., Karmakar, N. C., Pandey, S. K., et al. (2000). Novel biodegradable flocculants based on polysaccharides. *Current Science*, *78*, 798–803.

Siracusa, V., Ingrao, C., Giudice, A. L., Mbohwa, C., & Rosa, M. D. (2014). Environmental assessment of a multilayer polymer bag for food packaging and preservation: An LCA. *Food Research International*, *62*, 151–161.

Srivastava, A., O'Connor, I. B., Pandit, A., & Wall, J. G. (2014). Polymer-antibody fragment conjugates for biomedical applications. *Progress in Polymer Science*, *39*, 308–329.

Suvorova, A. I., Tyukova, I. S., & Trufanova, E. I. (2000). Biodegradable starch based polymeric materials. *Russian Chemical Reviews*, *69*, 451–459.

Wan, X., Li, Y., Wang, X., Chen, S., & Gu, X. (2007). Synthesis of cationic guar gum-graft-polyacrylamide at low temperature and its flocculating properties. *European Polymer Journal*, *43*, 3655–3661.

Wang, X. L., Yang, K. K., & Wang, Y. Z. (2003). Properties of starch blends with biodegradable polymers. *Journal of Macromolecular Science, C: Polymer Reviews*, *43*, 385–409.

Xie, C., Feng, Y., Cao, W., Xia, Y., & Lu, Z. (2007). Novel biodegradable flocculating agents prepared by phosphate modification of konjac. *Carbohydrate Polymers*, *67*, 566–571.

Xu, C., Luo, X., Lin, X., Zhuo, X., & Liang, L. (2009). Preparation and characterization of polylactide/thermoplastic konjac glucomannan blends. *Polymer*, *50*, 3698–3705.

Yadav, M., Sand, A., Mishra, M. M., Tripathy, J., Pandey, V. S., & Behari, K. (2012). Synthesis, characterization and applications of graft copolymer (κ-carrageenan-g-vinylsulfonic acid). *International Journal of Biological Macromolecules*, *50*, 826–832.

Zah, R., Hischier, R., Leão, A. L., & Braun, I. (2007). Curaua fibers in the automobile industry—A sustainability assessment. *Journal of Cleaner Production*, *15*, 1032–1040.